arXiv:cond-mat/0512589v2 [cond-mat.str-el] 28 Jul 2006

Metal–Insulator Transition Tuned by External Gates in Hall Systems with Constrictions

Emiliano Papa[1] and Tilo Stroh[2]
[1]*Department of Physics, University of Virginia, Charlottesville, VA 22904-4714*
[2]*Department of Physics, University of Siegen, 57068 Siegen, Germany*

(Dated: February 6, 2008)

The nature of a metal–insulator transition tuned by external gates in quantum Hall (QH) systems with point constrictions, as reported in recent experiments [S.Roddaro *et al.*, Phys. Rev. Lett. **95**, 156804 (2005)], is examined. We attribute this phenomenon to a splitting of the integer edge into conducting and insulating stripes, the latter wide enough to allow for the stability of the edge structure. Inter-channel impurity scattering and inter-channel Coulomb interactions do not destabilize this picture.

Introduction—A current interest in one-dimensional electron systems is driven in part by the advances in technology which have enabled fabrication of new materials and in part by a hope to observe the exotic effects predicted theoretically. In this context, the edge states of QH systems offer an especially attractive terrain for testing the properties of one-dimensional fermion states.

Even though remarkable theoretical progress has been achieved in understanding properties of Luttinger liquids (LL) [2, 3], some open problems remain on the experimental front [4, 5]. For instance, there are problems concerning the transport measurements across a constriction in a two-dimensional electron gas (2DEG) conducted by Roddaro *et al.* [1]. The theory [6, 7] predicts a change in the nature of linear transport across a backscattering point, depending on the value of the LL parameter: perfect transmission for attractive interactions across the sample and perfect reflection for repulsive interactions. For QH systems of bulk filling ν, at finite voltage the theory predicts the power-law left–right tunneling differential conductance $G \sim V^{2/\nu-2}$. Contrary to these expectations, measurements in QH samples at integer filling [1] reveal a metal–insulator transition across the point contact, tuned by the voltage of the top metallic gates, $V_{\rm g}$. The system is metallic at low $|V_{\rm g}|$ but becomes insulating at high $|V_{\rm g}|$. The bias-voltage evolution of constriction transmission in the latter case is similar to the one corresponding to bulk filling $\nu = 1/3$.

The low $|V_{\rm g}|$ behavior was examined in [8] and it was found that interedge repulsions across the gates can lead to suppression of quasi-particle backscattering at the constriction. In analogy, the insulating behavior of [1] at higher $|V_{\rm g}|$ (backscattering enhancement) would have been understood if electron interactions reversed sign at high $|V_{\rm g}|$, due in this case to the presence of image charges on the gates. Allowing for different potentials V_1, V_2 on the two 2DEG subsystems, and studying the change of the position of one of the edges upon variation of both of these voltages [9], we find that electron interedge interactions remain repulsive at any values of V_1 and V_2.

We examine then the structure of the QH edges surrounding the gates in presence of the magnetic field. As in the semi-infinite-gate case [10, 11], a sequence of compressible (CS) and incompressible (IS) stripes arises, but the geometry of these systems and $V_{\rm g}$ in [1] are nevertheless such the ISs and the CSs have comparable widths. The presence of ISs strongly influences the tunneling exponents, leading eventually to suppression of electron tunneling across the constriction.

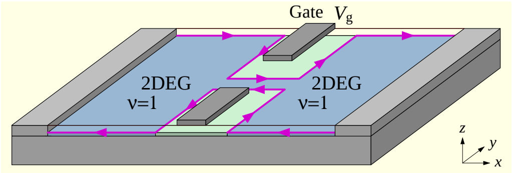

FIG. 1: Schematic illustration of a quantum Hall bar with a split-gate constriction. The gates bring counter-propagating edges in close proximity to enhance interedge backscattering.

The model—We consider here a QH system in which a point constriction with metallic gates, as in Fig. 1, has been created. The 2DEGs reside on the interface of two semiconductors, the xy plane ($z = 0$) of Fig. 1, and the gates over the top, a distance $10\, l_B$ ($l_B \approx 100\,$Å, the magnetic length) from the 2DEGs' plane, along the y axis of Fig. 1. We assume here that the system is homogeneous along the gates, the y direction, and that the gates and the 2DEGs are coplanar, an assumption justified at high $|V_{\rm g}|$. As $|V_{\rm g}|$ is increased, the electrons are repelled leaving behind positively charged dielectric stripes of lateral extension $a < |x| < b$, where $2a$ is the width of the gate region. In contrast to edges created by cleaved edge barriers [12] of width $\approx l_B$, the ones induced by gates are much wider, on the order of $\approx 30\, l_B$, with width growing quasi-linearly on $|V_{\rm g}|$. At higher $|V_{\rm g}|$ the edge structure becomes more complex than the simple single-channel chiral edge model. In absence of a magnetic field the configuration of the electrostatic potential in the 2DEGs' plane is $\phi(x) = V_{\rm g}$ in the gate region $|x| < a$ and $\phi(x) = V_1$ in the 2DEGs' regions, $|x| > b$. In addition, the positively charged dielectric in the depleted regions creates an electric field $E_z^{\rm str.}$ proportional to $\partial_z \phi(x, z) = 4\pi e n_0/\epsilon = \tau$ (in [1] donor charge density is $n_0 \approx 10^{11}\,{\rm cm}^{-2}$, and $\epsilon = 12.6$).

Nature of interactions—Intuitively one expects the presence of image charges in the gate, halfway between edges, to weaken the interedge Coulomb repulsions or even to reverse their sign. The system examined here, however, allows for exact calculations. To this end it is essential to allow for the 2DEG subsystems be at different potentials V_1 and V_2. The 2DEG edges $\bar{b}, b$ therefore are placed at different distances from the gate. The gate extends in $\bar{a} < x < a$, as illustrated

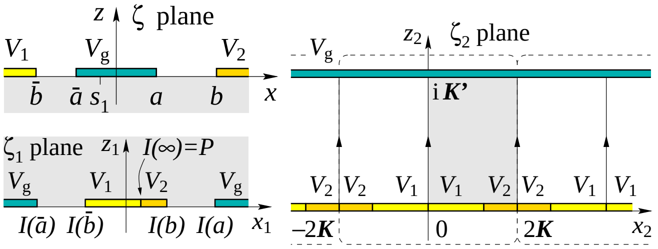

FIG. 2: Upper left: original potential configuration in space – metallic gate and 2DEG potential. Since $V_1 \neq V_2$ the distance 2DEGs–gate is different. Lower left: after inversion around a point s_1 the 2DEGs' distances from the gate are equal. Right: forming a box configuration (shaded) by mapping the upper ζ_1 half-plane, which in turn maps the lower half ζ plane (1). Application of the Schwarz mirroring principle about the vertical borders of the shaded box leads to a periodic structure along the x_2 axis.

in Fig. 2 (upper left).

To calculate the field created by the metallic components we use two conformal transformations. First, to get around the problem of $\bar{a} - \bar{b} \neq b - a$, we use an inversion I around a point s_1. The latter is defined such that in the inverted space the 2DEGs are at same distance from the gate, see Fig. 2 (left). Consecutively we use $\pi/2$ folding transformations at points $I(\bar{a}), I(\bar{b}), I(b), I(a)$ as follows,

$$\zeta_1 = \frac{R^2}{\zeta - s_1} + P \quad , \quad \zeta_2 = \mathrm{sn}^{-1}\left(\frac{\zeta_1}{I(b)}, \frac{I(b)}{I(a)}\right) + \boldsymbol{K} \quad , \tag{1}$$

where $\zeta_1 = I(\zeta)$, $\zeta = x + \mathrm{i}z$ etc., mapping the shaded parts of the spaces, see Fig. 2, onto each other. The radius of inversion, R, and the shift P just play intermediary roles yielding a scale-invariant potential. $\boldsymbol{K}$, $\boldsymbol{K}'$, $\boldsymbol{E}$, $\boldsymbol{E}'$ are the complete (complementary) Jacobi elliptic integrals of 1st and 2nd kind and sn^{-1} the inverse Jacobi elliptic function, each of modulus $k = I(b)/I(a)$, see also below.

To preserve the boundary conditions for the electric fields, i.e., $E_z^{\mathrm{el.}}(x; z = 0) = 0$ in the depleted regions $a < x < b$, $\bar{b} < x < \bar{a}$ of the original problem, we form the periodic configuration shown on Fig. 2 (right), obtaining at the box sides $E_{x_2}^{\mathrm{el.}}(x_2 = \pm 2n\boldsymbol{K}; z_2) = 0$, n integer.

The expression for the potential field $\phi^{\mathrm{el.}}(\zeta_2, \bar{\zeta}_2)$ can be calculated analytically, by summing up the series solution for the Laplace equation, to the close form

$$\phi^{\mathrm{el.}} = \tilde{V}_2 - \left(V_{\mathrm{g}} - \tilde{V}_2 - \frac{\tilde{V}_1 - \tilde{V}_2}{2\boldsymbol{K}} C\right) \frac{\mathrm{Re}\{\mathrm{i}\zeta_2\}}{\boldsymbol{K}'} + \frac{\tilde{V}_1 - \tilde{V}_2}{\pi} \mathrm{Re}\left\{\mathrm{i} \ln \frac{\vartheta_1\left(\frac{\pi}{4\boldsymbol{K}}(\zeta_2 + C), \mathrm{e}^{-\frac{\pi \boldsymbol{K}'}{2\boldsymbol{K}}}\right)}{\vartheta_1\left(\frac{\pi}{4\boldsymbol{K}}(\zeta_2 - C), \mathrm{e}^{-\frac{\pi \boldsymbol{K}'}{2\boldsymbol{K}}}\right)}\right\} \quad , \tag{2}$$

where ϑ_1 is a Jacobi theta function of modulus $k = S_k^-/S_k^+$ with $S_k^{\pm} = \left[(b - \bar{a})(a - \bar{b})\right]^{1/2} \pm \left[(b - a)(\bar{a} - \bar{b})\right]^{1/2}$, and $C = \zeta_2(I(\infty))$. Here $\tilde{V}_i = V_i - A$, $i = 1, 2$, with the shift caused by $E_x^{\mathrm{str.}}$ [13]. Due to the vanishing component $E_{x_2}^{\mathrm{el.}}$ along the lines $\zeta_2 = \pm 2n\boldsymbol{K} + \mathrm{i}z_2$, the Jacobian of the transformation $\zeta_2 \to \zeta$ simplifies to $J(2 \to 0) = -S_k^+/[2D(\zeta)]$, and in the unfolded space $E_x^{\mathrm{el.}}(x, z = 0) = \partial_{z_2}\phi^{\mathrm{el.}}(x_2, z_2) S_k^+/[2D(\zeta)]$, with $D(\zeta)$ given in [14].

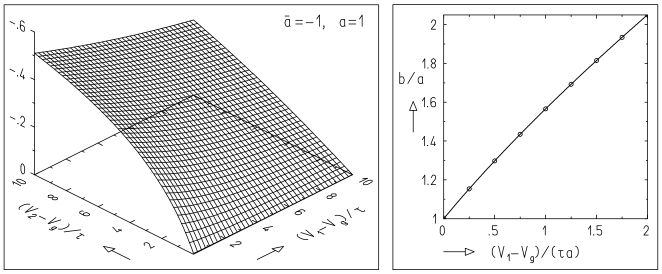

FIG. 3: Left: $\partial_{V_1}b/\partial_{V_2}b$, the ratio of the differential dependences of the edge position on the potentials on both sides of the gate. Right: dependence of the edge position b on $V_1 - V_{\mathrm{g}}$ for the symmetric case ($V_2 = V_1$; $\bar{a} = -a, \bar{b} = -b$).

For the calculation of the field created by the dielectric stripes we generalize an idea given by Glazman and Larkin [15] by representing the potential ϕ as the imaginary part of an analytic function F, which, by using the boundary conditions for its derivative, can be related to another function, $f(\zeta) = \mathrm{i}D(\zeta)(\mathrm{d}F/\mathrm{d}\zeta)$, whose imaginary part we would know everywhere along the x axis. By use of the Schwarz theorem one can generate $f(\zeta)$ on the whole plane. Here, for the uniformly charged asymmetric dielectric stripes one gets $f(\zeta) = \tau[\mathrm{i}D(\zeta) + \mathcal{F}(\zeta)]$, with $D(\zeta)$ and $\mathcal{F}(\zeta)$ given by [14]. One finds ϕ by taking the opposite steps, leading immediately to the value of the x component of the electric field, $E_x^{\mathrm{str.}} = \tau\mathcal{F}(x)/D(x)$.

From the equilibrium conditions of $E_x^{\mathrm{str.}}(x, z = 0) + E_x^{\mathrm{el.}}(x, z = 0) \to 0$ at $x \to \bar{b} + 0$ and $x \to b - 0$ one obtains the edge-position equations

$$\frac{b + \bar{b}}{2} = \frac{a + \bar{a}}{2} - \frac{V_1 - V_2}{\pi\tau} \, , \tag{3}$$

$$\frac{\tau}{2}(b - \bar{b})^2 = \frac{\tau}{2}\frac{\left(S_k^+\right)^2 \boldsymbol{E}'}{\boldsymbol{K}'} - \frac{S_k^+ V_0}{\boldsymbol{K}'} - \frac{V_1 - V_2}{\pi} l \, , \tag{4}$$

where $V_0 = V_{\mathrm{g}} - V_2 - (V_1 - V_2)C/(2\boldsymbol{K})$, and with l [16]. Treating numerically the transcendental equation for $\bar{b}, b$ to obtain $\partial_{V_1}b/\partial_{V_2}b$, we find that interactions remain repulsive at higher $|V_{\mathrm{g}}|$ as they do for low $|V_{\mathrm{g}}|$, Fig. 3 (left).

The edge position b, when $V_2 = V_1$, increases quasi-linearly with $|V_{\mathrm{g}}|$, $b \approx \kappa a[\ln(4\kappa/\mathrm{e}) - \ln\ln(4\kappa/\mathrm{e})]^{-1}$, where $\kappa = (V_1 - V_{\mathrm{g}})/\tau a$, as shown on Fig. 3 (right).

Edge structure—In the edge of a bulk integer filling $\nu = 1$ there exists a hierarchy of FQH energy gaps at fillings $f = p/(2mp \pm 1)$, for integers m and p. The system lowers its energy [10, 11, 17, 18] by relocating some electrons from higher to lower energies forming fractional-filling ISs around the points $x_{f\pm} = \pm b[(1 - k^2 f^2)/(1 - f^2)]^{1/2}$ of filling $n(x_{f\pm}) = fn_0$ where $n(x) = n_0[(x^2 - b^2)/(x^2 - a^2)]^{1/2}$. While a large number of alternating ISs and CSs can in principle form at the edge, only the widest few will be realized in

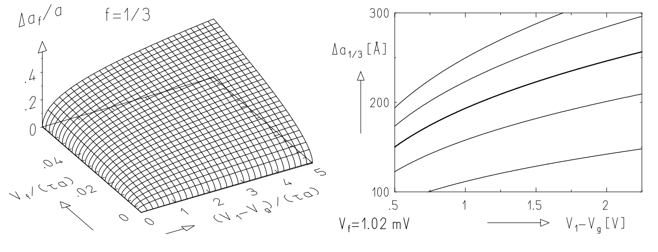

FIG. 4: Left: IS width $\Delta a_{1/3}$, in units of half-gate width, a. Right: IS width $\Delta a_{1/3}$, in Å as function of $V_1 - V_\mathrm{g}$ and V_f for the first-order approximation and the values $V_f \to (i/3)V_f$, $i = 1, \ldots, 5$, from bottom to top (in [1], $|V_1 - V_\mathrm{g}| = 0.7\,\mathrm{V}$, $a = 3000\,$Å).

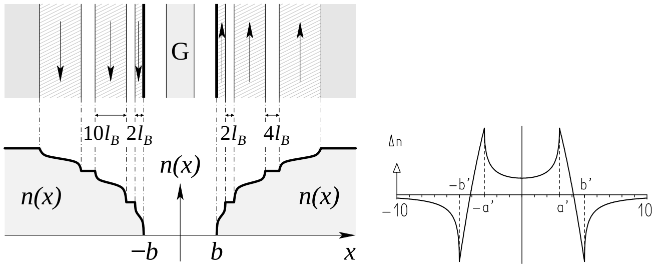

FIG. 5: Left: structure of the edge of a QH system surrounding a split gate, in presence of a strong magnetic field. Shaded areas notify current-carrying CSs, separated by insulating ISs. Right: magnified plot of additional electron charge caused by the magnetic field around the points $x_{f\pm}$ on the edge profile, $\Delta n = (n'_f/2x_f)[(a'^2+b'^2)/2 - x^2 \pm |D'(x)|]$, $(+)$ for $|x| > b'$, $(-)$ for $|x| < a'$, and zero otherwise.

practice. The largest charge gaps are known to occur at $f = 1/3, 2/3$ [18] and we calculate here the widths $\Delta a_{1/3}$, $\Delta a_{2/3}$.

In presence of a magnetic field, potential differences of value [10, 18] $V_f = 1.02\,\mathrm{mV} \ll |V_1 - V_\mathrm{g}|$ on the sides of the ISs $f = 1/3,\ 2/3$ arise. The charge density in the region of ISs, $\mathcal{N}(x) = n(x) - n_f$, should now be treated as x-dependent. Since $V_f/|V_1 - V_\mathrm{g}| \approx 10^{-3}$ [1], we can expand the even function $n(x)$ around the points $x_{f\pm}$ in one even polynomial $\sum_{i=0}^{N} \tilde{n}_i^{(N)} x^{2i}$ matching $n(x)$ up to the Nth derivative there. For $N = 2$, e.g., one gets $\{\tilde{n}_i^{(2)}\} = \{n_f - \frac{5}{8}x_f n'_f + \frac{1}{8}x_f^2 n''_f, \frac{3}{4}x_f^{-1}n'_f - \frac{1}{4}n''_f, -\frac{1}{8}x_f^{-3}n'_f + \frac{1}{8}x_f^{-2}n''_f\}$.

The potential field created by the charged stripes extended along $a' < |x| < b'$ with $a' > b$, found by integrating $f(\zeta)/D'(\zeta)$, $D'(\zeta) := D(\zeta)\{\bar{b}, \bar{a}, a, b \to -b', -a', a', b'\}$, along the real axis (of the general form $f(\zeta) = \tau[\mathrm{i}D'(\zeta) + \mathcal{F}(\zeta, a', b')]$), is now modified to account in principle for the nth order of approximation for $\mathcal{N}(x)$ [or $\tau(x) = (2\pi e/\epsilon)\mathcal{N}(x)$], $\tau_n(x) = \tau_n x^n$, giving for $\mathcal{F}$

$$\mathcal{F}_n = \tau_n \zeta^{n+2} \sum_{k=0}^{[n/2+1]} C_k^{-\frac{1}{2}}\left(\tfrac{a'^2+b'^2}{2a'b'}\right)\left(\frac{a'b'}{\zeta^2}\right)^k \quad , \tag{5}$$

where $C_k^{-\frac{1}{2}}(t)$ is a Gegenbauer polynomial, and $[\cdot]$ represents the integer part of a real number.

To second order, from conditions of equilibrium at both edges of the stripes, we find that a', b', in addition to the condition $a'^2 + b'^2 = 2x_f^2$, fulfill also

$$\frac{2-\bar{k}'^2}{2}\boldsymbol{E}' - (1-\bar{k}'^2)\boldsymbol{K}' = \frac{3\sqrt{2}}{4}(2-\bar{k}'^2)^{3/2}\frac{V_f}{\tau' x_f^2} \quad , \tag{6}$$

where $\bar{k} = a'/b'$, $\bar{k}'^2 = 1 - \bar{k}^2$. For the IS widths $\Delta a = b' - a'$ we find $\Delta a_f \approx \left[(16/\pi\tau) f V_f/(1-f^2)^{3/2}\right]^{1/2} b^{1/2}$, proportional to $V_\mathrm{g}^{1/2}$ up to logarithmic corrections. Numerical results for Δa_f are represented in Fig. 4. The narrower outer ISs are of size 180–200 Å, corrected upward in higher orders of expansion on $n(x)$. The wider inner $2/3$ channels, of size $\approx 400\,$Å, are $\approx 1000\,$Å away. These $(2\,l_B,\ 4\,l_B)$ are distances for which the overlap of electron wave functions on opposite sides of ISs is exponentially small. Therefore even the $1/3$ IS is insulating in the transversal direction at high $|V_\mathrm{g}|$.

Stability of edge structure—The dynamics of wide edges in strong magnetic fields, when the emerging ISs were assumed to be narrow, was studied in [19]. The excitation spectrum was found to be composed of an edge magnetoplasmon and slower-moving acoustic modes. In the latter charge density oscillates across the profile of the edge (x axis). The geometry of our system and the experimental values of V_g however are such that the 1/3 and 2/3 ISs of widths $2\,l_B$, $4\,l_B$ are of comparable size to the respective 1/3 and 2/3 CSs ($2\,l_B$, $10\,l_B$ wide), Fig. 5, and the model of coupled chiral LLs, is adopted below.

First of all, since the ISs, illustrated in Fig. 6, are wide, the effective statistics of fluctuating channels is the one characterizing the $\nu = 1/3$ edges [20]. In the absence of inter-channel Coulomb interactions, the LL formed between $\nu = 1/3$ channels at the line junction anticrossing the Hall bar is equivalent to a LL along the junction at filling $1/\nu$ [8, 21], a reflection of quasiparticle–electron duality in tunneling processes. Starting with an open constriction, slowly turning off V, the system flows from relevant quasiparticle backscattering, suppressing the source-to-drain conductance according to $G - \nu e^2/h \sim -V^{2\nu-2}$, to a closed constriction with irrelevant electron tunneling with $G \sim V^{2/\nu-2}$, unable to open the constriction at small V. The system is insulating at low bias with I–V characteristics of a QH system of bulk $\nu = 1/3$, in agreement with observations of Ref. [1].

Accounting for the inter-channel Coulomb interactions the action of same-chirality branches is

$$S = \sum_{i,j=1}^{3} \int \mathrm{d}x\,\mathrm{d}\tau \left[\frac{2\mathrm{i}\delta_{ij}}{\nu}\,\partial_\tau\phi_i\,\partial_x\phi_j + V_{ij}\,\partial_x\phi_i\,\partial_x\phi_j\right] \ , \tag{7}$$

where ϕ_i, $i = 1, 2, 3$, are bosonic fields associated with each CS. $\partial_x\phi_i = -\sqrt{\pi}\rho_i(x)$ is the charge density of channel i and quantization is assumed based on the commutation relations $[\rho_i(x), \rho_j(x')] = -\frac{\mathrm{i}\nu}{2\pi}\delta_{ij}\partial_x\delta(x - x')$. We can assume in general the intra-channel interactions V_{ii} for $i = 1, 2, 3$ to be different, and the inter-channel ones to fulfill $V_{ij} = V_{ji} \neq V_{ii}$. The diagonalized action can be written as

$$S = \sum_{i=1}^{3} \int \mathrm{d}x\,\mathrm{d}\tau \left[\frac{2\mathrm{i}}{\nu}(\partial_\tau\varphi_i)(\partial_x\varphi_i) + \lambda_i(\partial_x\varphi_i)^2\right] \ , \tag{8}$$

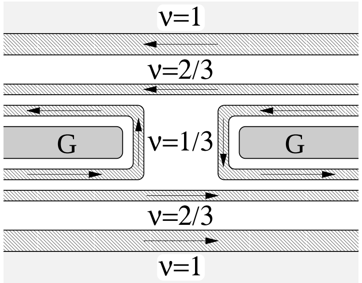

FIG. 6: Schematic illustration of high $|V_\mathrm{g}|$ splitting of an $\nu = 1$ edge into channels of fractional filling in QH systems with constriction, similar to the experiments of Ref. [1].

where $\varphi_i = M_{ij}\phi_j$ and λ_i are eigenvalues of V. Since all channels are of same chirality, the interaction-dependent M matrix is unitary, $(M^\dagger M)_{ij} = \delta_{ij}$, as opposed to $M^\dagger J M = J$, with $(J)_{ij} = \delta_{ij}\mathrm{sign}(j)$ in presence of opposite-chirality channels, resulting in $(M^\dagger M)_{ij} \neq \delta_{ij}$. The correlation functions between electrons, $R_i^{\mathrm{el.}} \sim \mathrm{e}^{\mathrm{i}\sqrt{4\pi}\phi_i/\nu}$, of branch i, have the form $\left\langle R_i^{\mathrm{el.}\dagger}(\tau) R_i^{\mathrm{el.}}(\tau')\right\rangle \sim \prod_{j=1}^{3}(\lambda_i(\tau - \tau'))^{-2(M^\dagger M)_{ij}/\nu}$, and the scaling dimensions are $d_i = \sum_j (M^\dagger M)_{ij}/\nu = 1/\nu$, irrelevant for $\nu = 1/3$ and unaffected by the interactions.

Another point of concern is the question of stability of the channel structure under inter-channel tunneling processes mediated by impurities along the edge. For repulsions $V_{ij} = V$ ($\leq V_{ii} = U$), the action is diagonalized in terms of two neutral and one charged field. At low energies the neutral fields tend to antilock charge densities in the consecutive channels. Inter-channel tunneling processes lead to the chiral sine-Gordon model $\cos(\frac{\sqrt{8\pi}}{\nu}\varphi_n)$, $n = 1, 2$, for neutral fields. The *cos* operator is relevant only for $\beta^2 \leq 16\pi$ [22], a condition not realized in these systems since $\beta^2 = 8\pi/\nu^2$ and $\nu = 1/3$.

As $|V_\mathrm{g}|$ is lowered we expect the $1/3$ IS channel to eventually close and the remaining $2/3$ IS to extend under the gate. At large bias, the same argument as in *high* $|V_\mathrm{g}|$ for the conductance applies, with $G - \nu e^2/h \sim -V^{2\nu-2}$ and $\nu = 2/3$. At low V, however, Coulomb interactions between opposite-chirality channels as discussed in [8] are expected to be strong leading to perfect transmission through the constriction and exhibiting the symmetry $\nu = 1/3 \leftrightarrow \nu = 2/3$ between the low and high $|V_\mathrm{g}|$ observed in the experiments of Ref. [1].

We are grateful to M. Grayson, V. Pellegrini, M. Polini, S. Roddaro for discussions and to A. MacDonald and A. Tsvelik for comments on the manuscript and discussions. This work was supported by NSF grant DMR-0412956.

---

[1] S. Roddaro *et al.*, Phys. Rev. Lett. **95**, 156804 (2005).

[2] A. O. Gogolin, A. Nersesyan, and A. M. Tsvelik, *Bosonization and Strongly Correlated Electrons*, Cambridge University Press, Cambridge, 1995.

[3] J. Voit, Rep. Prog. Phys. **58**, 977 (1995).

[4] M. Grayson *et al.*, Phys. Rev. Lett. **80**, 1062 (1998); M. Grayson *et al.*, Physica E **25**, 212 (2004);

[5] R. de-Picciotto *et al.*, Nature (London) **389**, 162 (1997); [Inspec] [ISI] Y. C. Chung *et al.*, Phys. Rev. B **67**, 201104(R) (2003); Phys. Rev. Lett. **91**, 216804 (2003).

[6] C. L. Kane and M. P. A. Fisher, Phys. Rev. B **46**, 15233 (1992); Phys. Rev. Lett. **68**, 1220 (1992);

[7] P. Fendley, A. W. W. Ludwig, and H. Saleur, Phys. Rev. Lett. **74**, 3005 (1995); Phys. Rev. B **52**, 8934 (1995).

[8] E. Papa and A. H. MacDonald, Phys. Rev. Lett. **93**, 126801 (2004); Phys. Rev. B **72**, 045324 (2005).

[9] The authors are grateful to Allan MacDonald for suggesting this idea on studying the nature of interactions.

[10] D. B. Chklovskii *et al.*, Phys. Rev. B **46**, 4026 (1992).

[11] D. B. Chklovskii *et al.*, Phys. Rev. B **47**, 12605 (1993).

[12] W. Kang *et al.*, Nature (London) **403**, 59 (2000); M. Huber *et al.*, Phy. Rev. Lett. **94**, 016805 (2005).

[13] Potential shift in (2): $A = \frac{\tau}{4} S_k^- \left(\frac{b-\bar{b}}{a-\bar{a}} + \frac{a-\bar{a}}{b-\bar{b}}\right) \boldsymbol{K}' - \frac{\tau}{2} S_k^+ \boldsymbol{E}'$.

[14] The functions D and $\mathcal{F}$ for asymmetric dielectric stripes are $D(\zeta) = [(\zeta - \bar{b})(\zeta - \bar{a})(\zeta - a)(b - \zeta)]^{1/2}$ and $\mathcal{F}(\zeta) = \frac{1}{2}(\zeta - \bar{b})(\zeta - b) + \frac{1}{2}(\zeta - \bar{a})(\zeta - a) - \frac{1}{8}(b - a - \bar{a} + \bar{b})^2$. This $\mathcal{F}$ is valid only for uniformly charged stripes.

[15] L. I. Glazman, I. A. Larkin, Semic. Sci. Tech. **6**, 32 (1991).

[16] The length l scaling the potential difference in (4) is $l = b - \bar{b} - 2\left[(a - \bar{b})(\bar{a} - \bar{b})\right]^{1/2} - S_k^+ \left(2E\left(\mathrm{am}\left(\frac{C}{2}\right)\right) - \frac{C\boldsymbol{E}}{\boldsymbol{K}}\right)$.

[17] C. W. J. Beenaker, Phys. Rev. Lett. **64**, 216 (1990).

[18] A. M. Chang, *The Quantum Hall Effect*, edited by R. Prange, S. M. Girvin, Springer-Verlag, New York, 1987.

[19] I.L. Aleiner *et al.*, Phys. Rev. Lett. **72**, 2935 (1994); S. Conti *et al.*, Phys. Rev. B **54**, 14309 (1996); M.D. Johnson *et al.* , Phys. Rev. B **67**, 205332 (2003).

[20] R. D'Agosta *et al.*, Phys. Rev. B **68**, 035314 (2003); Phys. Rev. Lett. **94**, 086801 (2005).

[21] S. R. Renn *et al.*, Phys. Rev. B **51**, 16832 (1995); C. L. Kane *et al.*, Phys. Rev. B **56**, 15231 (1997); L. Pryadko *et al.*, Phys. Rev. B **61**, 10929 (2000); E.-A. Kim *et al.*, Phys. Rev. B **67**, 045317 (2003); U. Zülicke *et al.*, Phys. Rev. B **69**, 085307 (2004); W.-C. Lee *et al.*, Phys. Rev. B **72**, 121304 (2005); A. Mitra *et al.*, Phys. Rev. B **64**, 041309 (2001).

[22] J. D. Naud *et al.*, Nucl. Phys. B **565**, 572 (2000).